

Accepted Article

Title: A Suite of "Minimalist" Photo-Crosslinkers for Live-Cell Imaging and Chemical Proteomics: Case Study with BRD4 Inhibitors

Authors: Shao Q. Yao, Sijun Pan, Se-Young Jang, Danyang Wang, Si Si Liew, Zhengqiu Li, and Jun-Seok Lee

This manuscript has been accepted after peer review and appears as an Accepted Article online prior to editing, proofing, and formal publication of the final Version of Record (VoR). This work is currently citable by using the Digital Object Identifier (DOI) given below. The VoR will be published online in Early View as soon as possible and may be different to this Accepted Article as a result of editing. Readers should obtain the VoR from the journal website shown below when it is published to ensure accuracy of information. The authors are responsible for the content of this Accepted Article.

To be cited as: *Angew. Chem. Int. Ed.* 10.1002/anie.201706076
Angew. Chem. 10.1002/ange.201706076

Link to VoR: <http://dx.doi.org/10.1002/anie.201706076>
<http://dx.doi.org/10.1002/ange.201706076>

COMMUNICATION

A Suite of “Minimalist” Photo-Crosslinkers for Live-Cell Imaging and Chemical Proteomics: Case Study with BRD4 Inhibitors

Sijun Pan, Se-Young Jang, Danyang Wang, Si Si Liew, Zhengqiu Li, Jun-Seok Lee* and Shao Q. Yao*

Abstract: Affinity-based probes (A/BPs) provide a powerful tool for large-scale chemoproteomic studies of drug-target interactions. The development of high-quality probes capable of recapitulating genuine drug-target engagement however could be challenging. “Minimalist” photo-crosslinkers, which contain an alkyl diazirine group and a chemically tractable tag, could alleviate such challenges, but few are currently available. Herein, we have developed new alkyl diazirine-containing photo-crosslinkers with different bioorthogonal tags. They were subsequently used to create a suite of A/BPs based on GW841819X (a small molecule inhibitor of BRD4). Through *in vitro* and *in situ* studies under conditions that emulated native drug-target interactions, we have obtained better insights into how a tag might affect the probe’s performance. Finally, SILAC-based chemoproteomic studies have led to the discovery of a novel off-target, APEX1. Further studies showed GW841819X binds to APEX1 and caused up-regulation of endogenous DNMT1 expression under normoxia conditions.

In drug discovery, lacks of efficacy and safety are two major causes of drug candidate attrition, which may be reduced by a more integrated understanding of the drug candidate in terms of its exposure, target engagement and pharmacological activities.^[1,2] Strategies based on small molecule probes have been introduced to facilitate studies of target engagement and identification, but they are not without major limitations.^[2-4] Ideally, such strategies should recapitulate drug-target interactions *in situ* (e.g. live cells) and allow for subsequent proteome-wide target enrichment/identification *in vitro* (from cell lysates).^[5] We recently named such approaches “*in situ* drug profiling”, which could trace its root to activity-based protein profiling (ABPP).^[6,7] For ABPP in which a reversible activity-based probe is used, since a photo-reactive moiety is needed in the probe design, such a probe is also called an “affinity-based probe” (A/BP).^[8] Given that non-covalent small molecules constitute > 90% of FDA-approved drugs, the development of high-quality A/BPs suitable for drug-target interaction studies in living cells is of paramount importance.^[3-14] In order to retain the original pharmacological properties of a non-covalent drug, chemical modifications on the parent compound should be made as small as possible.^[5,15] Based on recent systematic studies of A/BPs containing various

photo-reactive groups, alkyl diazirines have shown superior protein-labeling efficiency with low nonspecific labeling.^[16] On the other hand, given its small size and chemical stability, a terminal alkyne is an excellent tractable tag in the probe design, but the use of toxic Cu catalysts during Cu(I)-catalyzed azide-alkyne cycloaddition (CuAAC) makes it ill-suited for live-cell applications. The past decade has witnessed a remarkable expansion of tractable tags enabled by Cu-free bioorthogonal chemistries.^[17] Notwithstanding, such tags are uncommon in A/BPs, presumably due to the need of an additional photo-reactive group.^[18-20] Despite several elegant studies on the reactivity and selectivity of various bioorthogonal reactions,^[20-22] how significant a tag might affect the overall performance of an A/BP under “*in situ* drug profiling” settings has not been explored. We anticipated different bioorthogonal pairs would affect the proteome reactivity profiles of a probe, providing both drug- and tag-specific labeling patterns. Herein, we report the comprehensive cell-based proteome studies of GW841819X (a small molecule inhibitor of the epigenetic reader protein BRD4^[23]), by using a newly developed, diverse set of A/BPs containing a common alkyl diazirine and different tractable tags (Figure 1). We were hopeful that biased tag-specific signals caused by individual probes may be reduced, ultimately resulting in the emergence of true cellular targets (on and off) of the parent drug as common signals from all probes. This process was further combined with modern techniques in quantitative mass spectrometry (qMS), namely stable isotope labeling with amino acids in cell culture (SILAC) and neutron-encoded isobaric mass tag labeling (TMT10),^[24,25] to integrate various probes within a single experiment and reduce experimental errors associated with sample preparation and MS analysis (Figure S1).

We previously reported the first-generation “minimalist” photo-crosslinkers which consist of a small alkyl diazirine flanked by a terminal alkyne and various functional groups.^[26] They could be used to modify different bioactive compounds. Recently, one of these photo-crosslinkers was used to label GW841819X (renamed as **WT** in current study; Figure 1A), giving **BD-3**.^[27] When compared to a bulky photo-crosslinker (i.e. linker used in **BD-4**^[9]), such a “minimalist” design was shown to improve the performance of A/BPs. Subsequent attempts to replace the terminal alkyne with cyclopropene-containing tags, i.e. **BD-1** and **BD-2**, further enabled the *in situ* bioimaging capability by using the well-known tetrazine-cyclopropene ligation through an inverse electron demand Diels–Alder reaction (IEDDA).^[17] Despite being small in size and chemically accessible from the corresponding terminal alkyne, the relative chemical instability of cyclopropenes caused severe tag-specific background labeling in subsequent proteomic studies.^[17,27] Nevertheless, we found such imaging- and proteome profiling-enabled, dual-purpose probes could help in refining target identification by taking advantage of the subcellular distribution information attainable from imaging experiments. In the current study, we reasoned such issues may be further alleviated with additional A/BPs that contain different tractable tags in our chemoproteomic workflow (Figure S1).

[*] S. Pan, D. Wang, S. S. Liew, Prof. Dr. S. Q. Yao
Department of Chemistry, National University of Singapore,
3 Science Drive 3, Singapore 117543 (Singapore)
E-mail: chmyaosq@nus.edu.sg

[*] S.-Y. Jang, Prof. Dr. J.-S. Lee
Molecular Recognition Research Center, Bio-Med Program of KIST-
School UST, Korea Institute of Science & Technology,
Hwarangno 14-gil 5, Seongbuk-gu, Seoul 136-791, 136791 (Korea)
E-mail: junseoklee@kist.re.kr
Prof. Dr. Z. Li
College of Pharmacy, Jinan University, Guangzhou, 510632 (China)

Supporting information for this article is given via a link at the end of the document. ((Please delete this text if not appropriate))

COMMUNICATION

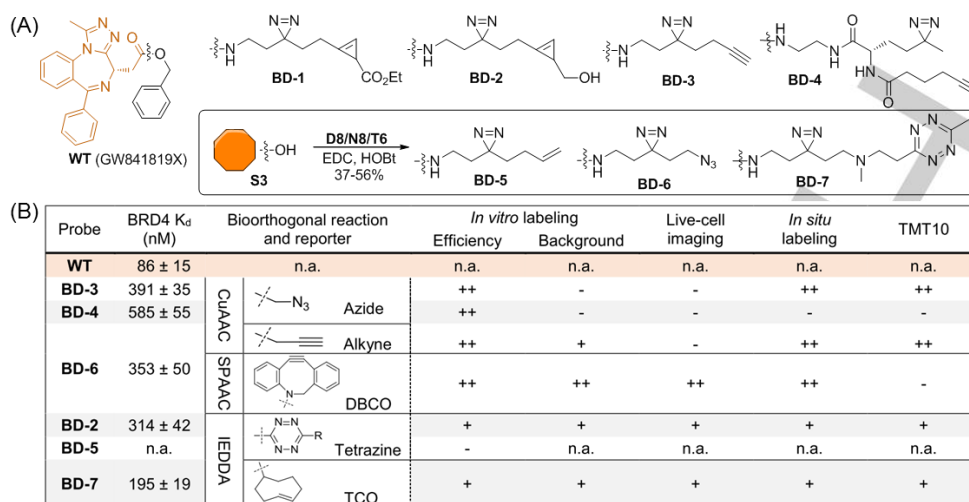


Figure 1. (A) Structures of various A/BPs based on GW841819X (WT), a recently discovered PPI inhibitor of BRD4,^[23] and (B) summary of their performance in various assays (*in vitro* labeling, live-cell imaging, *in situ* labeling & TMT10 qMS). Names of the “click” reactions and their fluorophore/biotin-containing reporters are shown (see Figures S2-S5 for full details). n.a. = Not available.

Similar to previously developed “minimalist” photo-crosslinkers, the new linkers (**D8**, **N8** and **T6** in Figure S3) consist of three key components: 1) a functional group (e.g. NH_2) that could be readily attached to a bioactive compound; 2) an alkyl diazirine, which is the smallest photo-reactive moiety that possesses excellent UV-induced protein labeling properties;^[12] and 3) a small chemically tractable tag for on-demand click chemistry. These components were joined together with short carbon chains. The tags in the current “minimalist” design, e.g. a terminal alkene, an aliphatic azide and a tetrazine, were chosen on the basis of their small sizes, chemical stability, robust bioorthogonality and scarcity in A/BPs. Terminal alkenes could be clicked to a tetrazine reporter via tetrazine-alkene ligation, although in general electron-rich or strained alkenes are needed.^[17,19] An aliphatic azide, despite initial concerns that it might be slowly reduced by intracellular thiols, was chosen because of its small size as well as wide applications in metabolic engineering.^[17] It could be clicked to either a terminal alkyne reporter via CuAAC, or a strained cyclooctyne via Cu-free strain-promoted azide-alkyne cycloaddition (SPAAC) in live cells.^[17,28] Finally, a small tetrazine tag was chosen over TCO because of its more favorable chemical and cellular stability.^[17] The resulting linkers, together with the previously reported bulky photo-crosslinker,^[9] were used to synthesize four new BRD4-targeting A/BPs, **BD-4**, **BD-5**, **BD-6**, and **BD-7**. They were then combined with two previously reported probes (**BD-2** and **BD-3**^[27]), to create a suite of A/BPs for comprehensive proteome profiling studies (Figure 1).

BRD4, a bromodomain-containing protein that recognizes acetylated lysine (Kac) residues such as those located on histones, is an important epigenetic “reader” involved in numerous critical cellular processes.^[29] Previous proteomic studies, with either an immobilized probe and cells lysates or A/BPs (i.e. **BD-2** and **BD-3**) under *in situ* conditions,^[23,27] could be ineffective due to the aforementioned reasons. With all six BRD4-targeting A/BPs in hand, including **BD-2/BD-3** (**BD-1** was not used due to its poor labeling property^[27]) and the newly synthesized **BD-4/BD-5/BD-6/BD-7**, the overall performance of this suite of probes was evaluated through a panel of *in vitro* and

cell-based assays with a focus on target binding and labeling, and results are summarized in Figure 1B. By comparing these A/BPs in various settings relevant to “*in situ* drug profiling”, we showed the choice of tags in an A/BP indeed played a significant role in determining the probe’s performance both *in vitro* (Figures S6-S8) and in live-cell environments (Figures 2 & S9).

In vitro labeling experiments with BRD4-overexpressing bacterial lysates showed UV-dependent, positive target labeling with all probes except **BD-5** at 0.2 μM (Figure S6). Addition of **WT** (10x) abolished the labeling. Negative BRD4 labeling by **BD-5** was attributed to a much lower reactivity between tetrazine and a simple alkene compared to other click reactions.^[17] **BD-5** was therefore not investigated further. Isothermal titration calorimetry (ITC) experiments to measure direct probe-target binding indicated the K_d values of all probes were within 3-5 folds of that of **WT**, with the exception of **BD-4**. Of note, in addition to the linker size as a primary concern, modifications of the ester linkage (to an amide) and the benzyl moiety (to an alkyl linker) might affect the physicochemical properties (e.g., hydrophobicity, H-bonding ability) of the probes and hence their binding affinities. We reasoned that these limitations could be outweighed by the convenient preparation of small A/BPs by using our “minimalist” linkers. We next investigated the cellular effects of these probes on endogenous BRD4 activities. Inhibition of BRD4 was previously shown to cause transcriptional down-regulation of *c-Myc*.^[23,29] As shown in Figure 2A, cells treated with **WT** or one of the A/BPs showed apparent inhibition of *c-Myc* with **WT** being the most effective inhibitor, followed by **BD-7** > **BD-3** \approx **BD-6** > **BD-2** \approx **BD-4**. This order was similar but clearly not identical to the relative BRD4-binding affinity obtained from *in vitro* ITC results. More pronounced differences in cellular activities of the A/BPs might have resulted from additional differences in their cell permeability, subcellular distribution and off-targeting. To more directly probe the on-target interaction of our A/BPs in live cells, *in situ* proteome labeling followed by PD/Western blotting (WB) were performed (Figures 2B & S9); the 152-kDa BRD4 band was successfully detected in probe-labeled cells but not in cells pre-treated with **WT** (10x). **BD-4** showed very weak *in situ* BRD4

COMMUNICATION

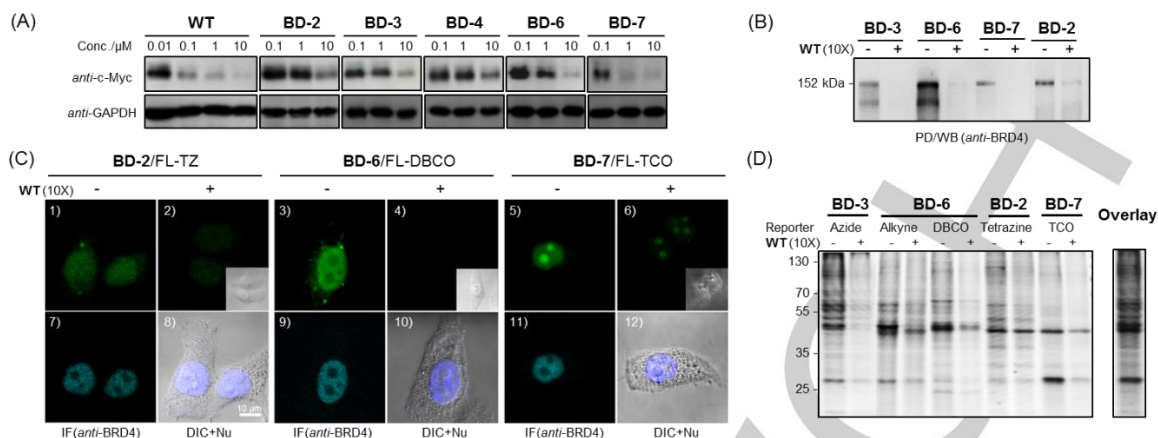


Figure 2. Probe performance in live-cell conditions. (A) Western blotting (WB) analysis of endogenous c-Myc expression level in MV4-11 cells treated with WT/probe at indicated concentrations (for 24 h). (Bottom gels): GAPDH loading control. (B) PD/WB studies of endogenous BRD4 (i.e. the 152-kDa bands) from live HepG2 cells. Cells were *in situ*-labeled with a probe (5 μ M for 3 h, \pm 10x WT). (C) Live-cell imaging with BD-2/BD-6/BD-7 (5 μ M, 37 $^{\circ}$ C for 3 h \pm 10x WT) in HepG2 cells. Upon probe treatment/UV irradiation, live-cell click reaction with a cell-permeable reporter (FL-TZ1, FL-DBCO or FL-TCO, respectively, 25 μ M for 1 h) was done followed by image acquisition under indicated reporter channel. Where applicable, immunofluorescence (IF) and nuclear staining were carried out. Nu = Hoechst channel; IF was done with anti-BRD4 antibody. Scale bar = 10 μ m. (D) In-gel fluorescence scanning profiles of live HepG2 cells labeled with an indicated probe (5 μ M for 3 h, \pm WT). (Lane 11): overlaid picture of lanes 1/3/5/7/9.

Labeling, presumably due to its bulky photo-crosslinker (Figure S9). These results, together with earlier findings that **BD-4** had weak cellular activities, highlight the need to carefully consider the size of a photo-crosslinker in an A/BP design. Encouragingly, we found two newly developed probes, **BD-6** and **BD-7**, were effective A/BPs for *in situ* labeling of endogenous BRD4, and therefore suitable in subsequent proteome profiling experiments. We previously showed **BD-2**, but not **BD-3**, was suited for live-cell imaging. **BD-6** and **BD-7** were designed to have similar capabilities as their tags may be tracked by Cu-free bioorthogonal chemistries (Figure 1B). As shown in Figure 2C, similar to **BD-2**, which upon being clicked to FL-TZ1 could be used to image nuclear-localized BRD4 in live cells, comparable results were obtained with **BD-6/FL-DBCO** and **BD-7/FL-TCO** pairs; probe-treated cells showed strong fluorescence throughout cell nuclei (panels 1/3/5), and **BD-6** particularly colocalized well with signals from immunofluorescence (IF) experiments using anti-BRD4 antibody (panels 3/9). Interestingly, each probe displayed distinct nuclear-localized staining patterns; while **BD-2** signals were evenly distributed throughout the entire nucleus (panel 1), signals from **BD-6** (panel 3) and **BD-7** (panel 5), in sharp contrast, avoided and concentrated in the region of nucleoli, respectively. It should be noted that the nucleolus-avoiding **BD-6** signals were akin to those from IF experiments (compare panels 3 & 9). This indicates **BD-6** might be the best-performing BRD4-imaging probe. Finally, we performed gel-based *in situ* proteome profiling (Figure 2D); similar WT-dependent proteome labeling profiles from all four probe-treated cells were obtained. As previously observed with **BD-3**,^[27] the fluorescent labeling of endogenous BRD4 was not distinct in **BD-2/BD-6/BD-7** treated samples, presumably due to its low expression level. Among the probes, the labeling profile of **BD-7** appeared most distinct (lane 9), while **BD-3** displayed the lowest non-specific labeling (compare lanes 1 & 2). We further performed *in vitro* lysate labeling experiments to compare background labeling profiles arising from various reporters (Figure S9). Finally, aggregate labeling patterns were generated by overlaying the various proteome labeling profiles (-

WT; lane 11 in Figure 2D), which could be treated as a reasonable representation of the complete drug-target engagement profile of WT from this suite of A/BPs. The overlaid gel was similar to that of **BD-3**, indicating **BD-3** might be one of the most suitable A/BPs for subsequent target identification.

Having obtained a comprehensive picture of various A/BPs, we summarized their performance in Figure 1B with the following recommendations: (1) for *in vitro* and *in situ* proteome profiling, where click chemistry is carried out post-UV irradiation under *in vitro* conditions, terminal alkyne- and azide-containing photo-crosslinkers (e.g. in **BD-3/BD-6**) are ideal, as both tags are small and give minimum background labeling. Probes such as **BD-2** and **BD-7** might be suitable, but their performance could be compromised by nonspecific labeling; (2) for live-cell imaging, photo-crosslinkers having a suitable cyclopropene, N₃ or tetrazine (e.g. in **BD-2/BD-6/BD-7**) may be used to provide additional information on drug-target interaction at subcellular levels; (3) in cases where both live-cell imaging and *in situ* proteome profiling are carried out, N₃-containing A/BPs might be the most ideal (e.g. **BD-6**), providing the best compromise in size, stability and bioorthogonality.

Unlike standard LC-MS/MS experiments,^[27] quantitative mass spectrometry (qMS) such as SILAC and TMT could minimize intrinsic variations during sample preparation and MS analysis, thus delivering more accurate protein hits in a chemoproteomic workflow. The TMT10 approach can analyze up to 10 MS samples in a single run, but requires labeling of post-PD peptides at the final stage prior to MS analysis. In the current work, although it was well-suited for simultaneous comparison of our A/BPs (Figure S10), we found significant discrepancies in the resulting MS data when compared to live-cell imaging results. Nevertheless, we were able to conclude that, as earlier discussed, **BD-3/BD-6** were the most suitable A/BPs for target identification (Figure 1B). SILAC on the other hand, despite its limited multiplicity, introduces isotopes into proteins at the start of the workflow, and thus is well-suited for subsequent *in vitro* PD/MS analysis which requires multi-step sample preparations. Therefore, **BD-3** and **BD-6** were

COMMUNICATION

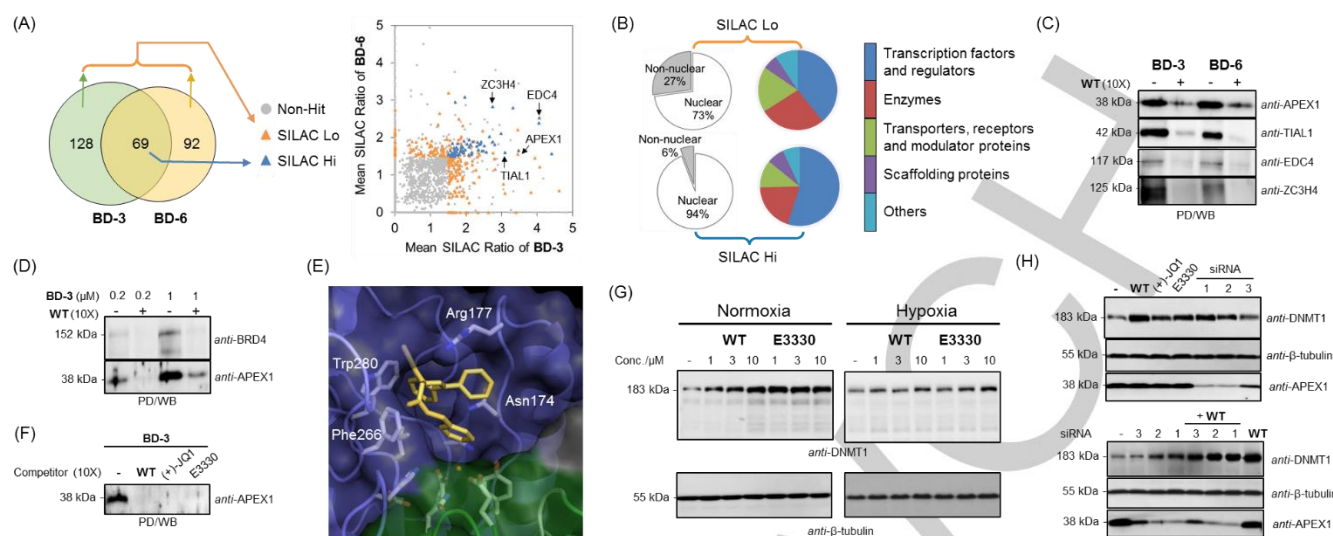


Figure 3. (A) Venn diagram and SILAC plot of preferred hits, with “SILAC Hi” and “SILAC Lo” shown in blue and orange, respectively. (B) Nuclear localization and functional classes of “SILAC Hi” and “SILAC Lo” in (A). (C) PD/WB studies of endogenous candidate proteins in HepG2 cells, *in situ* labeled with **BD-3**/**BD-6** (5 μ M), with or without **WT**. (D) Same as (C) except **BD-3** concentration was varied (0.2 or 1 μ M). (E) Docked structure of **WT** (yellow) in the active site of the DNA repair domain in APEX1 (PDB ID: 5DG0). (F) Same as (C) by using **BD-3** (5 μ M), and with either **WT**, (+)-JQ1 or E3330 as a competitor (10X). (G) WB analysis of endogenous DNMT1 expression level (top gels) of HepG2 cells upon treated with **WT** or E3330 at an indicated concentration (0, 1, 3, 10 μ M) for 24 h under normoxia or hypoxia conditions. (Bottom gels): β -tubulin as loading control. (H) Same as (G) except the cells were transfected with one of the three APEX1 siRNAs (see Supplementary Information for details) or treated with an inhibitor (10 μ M) (top gels). (Bottom gels): effects on APEX1-knockdown cells without and with treatment of **WT** (10 μ M).

chosen in the following SILAC experiments. Following previously established protocols,^[30] a protein was designated as a hit if: 1) it exhibited SILAC ratios ≥ 1.5 in both Forward and Reverse experiments, or 2) the mean value of the two SILAC ratios ≥ 1.5 with coefficient of variation (CV) < 0.67 (Figure S10). Such filters revealed 197 and 161 protein hits enriched by **BD-3** and **BD-6**, respectively, with 69 common targets designated as “SILAC Hi” (Figure 3A). The remaining 220 protein hits enriched by only one of the two A/BPs were designated as “SILAC Lo”. Further analysis of both sets of hits indicates 94% and 73% of them are found in the nucleus (Figure 3B), which corroborates with earlier live-cell imaging results. Further functional class analysis of “SILAC Hi” hits revealed most hits belong to transcription factors and regulators. Finally, we found 11 of the “SILAC Hi” hits and 12 of the “SILAC Lo” hits possess structural similarities with BRD4, with many known to interact with BRD4 and/or its inhibitors (Table S1). Further ranking identified four highest-confidence, nuclear-localized hits as likely true off-targets of **WT** (Table S2). Preliminary validation on these hits showed all of them were labeled by both probes in an activity-based manner in live cells (Figure 3C). Among them, APEX1 (an enzyme containing a redox and a DNA repair domain) immediately caught our attention due to its well-documented therapeutic potential for various diseases.^[31] We first ensured that endogenous APEX1 was successfully labeled by **BD-3** at a physiologically relevant probe concentration (Figure 3D); with 0.2 μ M of **BD-3**, stronger labeling of endogenous APEX1 over BRD4 was detected, indicating in the same drug-treated cells, **WT** might engage APEX1 preferentially over its intended target BRD4. This is a clear sign of off-targeting. A well-known small molecule inhibitor of APEX1, E3330 (Figure S11), was found to bind to the enzyme’s repair active site.^[32] Docking results showed **WT** also fits snugly in the repair active site of APEX1, with the triazolodiazepine moiety located inside the

enzyme’s pocket bordered by Arg¹⁷⁷/Phe²⁶⁶/Trp²⁸⁰ (Figure 3E). Other binding sites on APEX1 (e.g. the redox domain) however could not be excluded for possible **WT** interactions. Further competitive PD/WB studies confirmed that **WT** indeed occupied the same binding site on APEX1 as E3330, as well as (+)-JQ1 (another BRD4 inhibitor that is analogous to **WT**; Figure 3F). To further substantiate direct **WT**-APEX1 engagement in cells, which might lead to modulation of the enzyme’s cellular activities, we carried out a cell-based assay to monitor endogenous DNMT1 expression. APEX1 was previously shown to be inhibited by E3330 leading to DNMT1 up-regulation in epithelial stem cells.^[33] Similar cellular effects were observed in HepG2 cells treated with **WT**, E3330 or (+)-JQ1 (Figure 3G & S11); both **WT** and E3330 caused an apparent increase in DNMT1 expression at 10 μ M under normoxia conditions. Such an effect was attenuated under hypoxia conditions. Our finding thus suggests **WT** could mimic the cellular activities of E3330, presumably through inhibition of endogenous APEX1. Further siRNA knockdowns of APEX1 showed a similar increase in DNMT1 expression, which was consistent with previous studies (Figure 3H);^[33] the effect was directly relevant to the level of APEX1 down-regulation, with more complete knockdown of APEX1 resulting in a higher DNMT1 expression. Finally, addition of **WT** to the APEX1-knocked down cells further enhanced the up-regulation of DNMT1, presumably through the effective inhibition of the remaining APEX1 activities that were responsible for DNMT1 regulation.

Our pursuit of “minimalist” photo-crosslinkers has led to the successful development of new alkyl diazirine-containing linkers with a variety of bioorthogonal tags, which were subsequently used to generate a suite of A/BPs. By conducting comprehensive studies under conditions that emulated native drug-target interactions, we have obtained a clear view of how a tag might affect the overall performance of a probe. By employing

COMMUNICATION

quantitative mass spectrometry with select probes, we have conducted chemoproteomic studies for GW841819X, and successfully identified APEX1 as a novel off-target. Subsequent cell-based assays indicated GW841819X was able to bind to APEX1 in HepG2 cells and caused up-regulation of endogenous DNMT1 expression under normoxia conditions.

Acknowledgements

Funding was provided by National Medical Research Council (CBRG/0038/2013), Singapore, KIST (2E26632/2E26110, CAP-16-02-KIST) and the Bio & Medical Technology Development Program of the National Research Foundation (NRF-2016M3A9B6902060) from Ministry of Science, Korea.

Keywords: affinity-based probe • photo-crosslinker • bioorthogonal chemistry • live-cell imaging • epigenetics

- [1] P. Morgan, P. H. Van der Graaf, J. Arrowsmith, D. E. Feltner, K. S. Drummond, C. D. Wegner, S. D. A. Street, *Drug Discov. Today* **2012**, *17*, 419-424.
- [2] M. Schurmann, P. Janning, S. Ziegler, H. Waldmann, *Cell Chem. Biol.* **2016**, *23*, 435-441.
- [3] M. E. Bunnage, E. L. P. Chekler, L. H. Jones, *Nat. Chem. Biol.* **2013**, *9*, 195-199.
- [4] G. M. Simon, M. J. Niphakis, B. F. Cravatt, *Nat. Chem. Biol.* **2013**, *9*, 200-205.
- [5] Y. Su, J. Ge, B. Zhu, Y.-G. Zheng, Q. Zhu, S. Q. Yao, *Curr. Opin. Chem. Biol.* **2013**, *17*, 768-775.
- [6] M. J. Niphakis, B. F. Cravatt, *Annu. Rev. Biochem.* **2014**, *83*, 341-377.
- [7] L. E. Sanman, M. Bogoy, *Annu. Rev. Biochem.* **2014**, *83*, 249-273.
- [8] E. W. S. Chan, S. Chattopadhyaya, R. C. Panicker, X. Huang, S. Q. Yao, *J. Am. Chem. Soc.* **2004**, *126*, 14435-14446.
- [9] H. Shi, C.-J. Zhang, G. Y. J. Chen, S. Q. Yao, *J. Am. Chem. Soc.* **2012**, *134*, 3001-3014.
- [10] P. Ranjitkar, B. G. K. Perera, D. L. Swaney, S. B. Hari, E. T. Larson, R. Krishnamurthy, E. A. Merritt, J. Villen, D. J. Maly, *J. Am. Chem. Soc.* **2012**, *134*, 19017-19025.
- [11] J. J. Hulce, A. B. Coggnetta, M. J. Niphakis, S. E. Tully, B. F. Cravatt, *Nat. Methods* **2013**, *10*, 259-264.
- [12] S. Pan, H. Zhang, C. Wang, S. C. L. Yao, S. Q. Yao, *Nat. Prod. Rep.* **2016**, *33*, 612-620.
- [13] M. H. Wright, S. A. Sieber, *Nat. Prod. Rep.* **2016**, *33*, 681-708.
- [14] J. Park, M. Koh, S. B. Park, *Mol. BioSyst.* **2013**, *9*, 544-550.
- [15] S. Ziegler, V. Pries, C. Hedberg, H. Waldmann, *Angew. Chem. Int. Ed.* **2013**, *52*, 2744-2792.
- [16] P. Kleiner, W. Heydenreuter, M. Stahl, V. S. Korotkov, S. A. Sieber, *Angew. Chem. Int. Ed.* **2017**, *56*, 1396-1401, and references cited therein.
- [17] D. M. Patterson, L. A. Nazarova, J. A. Prescher, *ACS Chem. Biol.* **2014**, *9*, 592-605.
- [18] K. S. Yang, G. Budin, T. Reiner, C. Vinegoni, R. Weissleder, *Angew. Chem. Int. Ed.* **2012**, *51*, 6598-6603.
- [19] C. Li, T. Dong, Q. Li, X. Lei, *Angew. Chem. Int. Ed.* **2014**, *53*, 12111-12115.
- [20] A. Rutkowska, D. W. Thomson, J. Vappiani, T. Werner, K. M. Mueller, L. Dittus, J. Krause, M. Muelbaier, G. Bergamini, M. Bantscheff, *ACS Chem. Biol.* **2016**, *11*, 2541-2550.
- [21] L. I. Willems, N. Li, B. I. Florea, M. Ruben, G. A. van der Marel, H. S. Overkleeft, *Angew. Chem. Int. Ed.* **2012**, *51*, 4431-4434.
- [22] H. E. Murrey, J. C. Judkins, C. W. am Ende, T. E. Ballard, Y. Fang, K. Riccardi, L. Di, E. R. Guilmette, J. W. Schwartz, J. M. Fox, D. S. Johnson, *J. Am. Chem. Soc.* **2015**, *137*, 11461-11475.
- [23] C.-W. Chung, H. Coste, J. H. White, O. Mirguet, J. Wilde, R. L. Gosmini, C. Delves, S. M. Magny, R. Woodward, S. A. Hughes, E. V. Boursier, H. Flynn, A. M. Bouillot, P. Bamborough, J.-M. G. Brusq, F. J. Gellibert, E. J. Jones, A. M. Riou, P. Homes, S. L. Martin, I. J. Uings, J. Toum, C. A. Clement, A.-B. Boullay, R. L. Grimley, F. M. Blande, R. K. Prinjha, K. Lee, J. Kirilovsky, E. Nicodeme, *J. Med. Chem.* **2011**, *54*, 3827-3838.
- [24] S.-E. Ong, Mann, M. *Nat. Protocols* **2007**, *1*, 2650-2660.
- [25] T. Werner, G. Sweetman, M. F. Savitski, T. Mathieson, M. Bantscheff, M. M. Savitski, *Anal. Chem.* **2014**, *86*, 3594-3601.
- [26] Z. Li, P. Hao, L. Li, C. Y. J. Tan, X. Cheng, G. Y. J. Chen, S. K. Sze, H.-M. Shen, S. Q. Yao, *Angew. Chem. Int. Ed.* **2013**, *52*, 8551-8556.
- [27] Z. Li, D. Wang, L. Li, S. Pan, Z. Na, C. Y. J. Tan, S. Q. Yao, *J. Am. Chem. Soc.* **2014**, *136*, 9990-9998.
- [28] J. Z. Yao, C. Uttamapinant, A. Poloukhine, J. M. Baskin, J. A. Codelli, E. M. Sletten, C. R. Bertozzi, V. V. Popik, A. Y. Ting, *J. Am. Chem. Soc.* **2012**, *134*, 3720.
- [29] P. Filippakopoulos, S. Knapp, *Nat. Rev. Drug Discov.* **2014**, *13*, 339-358.
- [30] D. Wang, S. Du, A. Cazenave-Gassiot, J. Ge, J.-S. Lee, M. R. Wenk, S. Q. Yao, *Angew. Chem. Int. Ed.* **2017**, *56*, 5829-5833.
- [31] G. Kaur, R. P. Cholia, A. K. Mantha, R. Kumar, *J. Med. Chem.* **2014**, *57*, 10241-10256.
- [32] J. Zhang, M. Luo, D. Marasco, D. Logsdon, K. A. LaFavers, Q. Chen, A. Reed, M. R. Kelley, M. L. Gross, M. M. Georgiadis, *Biochemistry* **2013**, *52*, 2955-2966.
- [33] G. Chen, J. Chen, Z. Yan, Z. Li, M. Yu, W. Guo, W. Tian, *Sci. Rep.* **2017**, *7*: 40762.

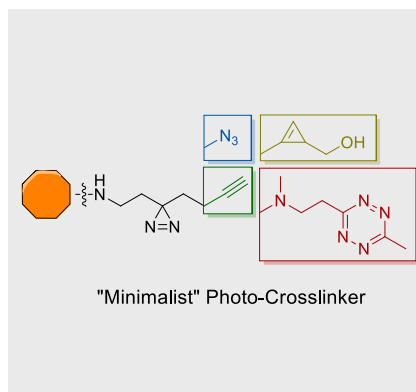
COMMUNICATION

Entry for the Table of Contents (Please choose one layout)

Layout 1:

COMMUNICATION

Tagging for More. New “minimalist” alkyl diazirine-containing photo-crosslinkers with different bioorthogonal tags were developed, and used to create a suite of AfBPs based on a known small molecule inhibitor of BRD4.



S. Pan, S.-Y. Jang, D. Wang, S. S. Liew,
Z. Li, J.-S. Lee,* Shao Q. Yao*

Page No. – Page No.

A Suite of “Minimalist” Photo-Crosslinkers for Live-Cell Imaging and Chemical Proteomics: Case Study with BRD4 Inhibitors